International Journal of Cardiology 289 (2019) 131–137

Contents lists available at ScienceDirect

International Journal of Cardiology

journal homepage: www.elsevier.com/locate/ijcard

Association between asymmetric dimethylarginine and in-stent restenosis tissue characteristics assessed by optical coherence tomography☆

Wei-Chieh Huang [a,b,c], Hsin-I Teng [d], Hsiang-Yao Chen [a,b], Ching-Ju Wu [a,b], Chuan-Tsai Tsai [a,b], Chien-Hung Hsueh [a], Ying-Ying Chen [e], William K. Hau [f], Tse-Min Lu [a,b,g,*]

[a] Division of Cardiology, Department of Internal Medicine, Taipei Veterans General Hospital, Taipei, Taiwan, ROC
[b] Department of Internal Medicine, School of Medicine, College of Medicine, National Yang Ming University, Taipei, Taiwan, ROC
[c] Division of Cardiology, Department of Internal Medicine, New Taipei City Hospital, New Taipei City, Taiwan, ROC
[d] Division of Cardiology, Chia-Yi & Wan-Qiao Branch, Taichung Veterans General Hospital, Taichung, Taiwan, ROC
[e] Division of Nephrology, Department of Internal Medicine, MacKay Memorial Hospital, Taipei, Taiwan, ROC
[f] Department of Medicine and Therapeutics, The Chinese University of Hong Kong, Hong Kong Special Administrative Region
[g] Department of Health Care Center, Taipei Veterans General Hospital, Taipei, Taiwan, ROC

ARTICLE INFO

Article history:
Received 19 November 2018
Received in revised form 8 April 2019
Accepted 2 May 2019
Available online 3 May 2019

Keywords:
Asymmetric dimethylarginine
In-stent restenosis
Optical coherence tomography
Neoatherosclerosis

ABSTRACT

Background: Impaired bioavailability of endothelium-derived nitric oxide (NO) and endothelial dysfunction may play a pivotal role in the pathogenesis of in-stent restenosis (ISR) after coronary stenting. We aimed to investigate the relation between asymmetric dimethylarginine (ADMA), an endogenous NO synthase inhibitor, and the ISR lesions tissue characteristics assessed by optical coherence tomography (OCT).

Methods and results: Forty-five patients with symptomatic ISR lesions (17 bare metal stents, 28 drug-eluting stents, medium implantation duration: 58.0 months) were evaluated by OCT for in-stent tissue characteristics and calcification. We defined neoatherosclerosis as the presence of lipid or calcified neointima in ISR lesions, and 12 (26.7%), 33 (73.3%) ISR lesions were classified as with homogenous neointima and neoatherosclerosis respectively. The patients with neoatherosclerosis have significantly higher plasma ADMA levels compared to those of patients with homogenous neointima (1.12 ± 0.21 μmol/l versus 0.83 ± 0.08 μmol/l, $p < 0.001$). Furthermore, the plasma ADMA level of ISR lesions with intra-stent calcification ($n = 24$, 53.3%) was also significantly higher than those of ISR lesions without ($n = 21$, 46.7%; $p < 0.001$). There was a highly significant association between plasma ADMA level and intra-stent relative calcium index (mean calcium arc × calcium length)/(360 × analyzed length) ($p < 0.001$, $r = 0.702$). In multivariate analyses adjusted for age, sex, diabetes, eGFR, plasma ADMA level remained the only significant predictor for the presence of neoatherosclerosis ($p = 0.008$) and intra-stent calcification ($p < 0.001$). In contrast, plasma ADMA level correlated with intra-stent relative lipid core index (mean lipid core arc × lipid core length)/(360 × analyzed length) only in subgroup without intra-stent calcification ($p = 0.004$, $r = 0.596$, multivariate-adjusted $p = 0.022$).

Conclusions: Increased plasma ADMA levels were associated with the development of in-stent neoatherosclerosis and calcification.

1. Introduction

In-stent restenosis (ISR) is a common complication after coronary stenting. Although the introduction of new-generation drug-eluting stent (DES) has greatly reduced the neointimal proliferation and risk of ISR, late stent failure still raises some concern after the placement of stent. Recent pathology studies have suggested that in-stent neoatherosclerosis may be a potential contributing factor of late ISR and late/very late stent thrombosis [1,2]. The development of in-stent neoatherosclerosis seems to occur early in months to years after the implantation of stent, especially DES; and have been reported to be caused by poor re-endothelialization and incompetent endothelium after coronary stenting [3]. Impaired bioavailability of endothelium-derived nitric oxide (NO) and endothelial dysfunction may play a pivotal role in the pathogenesis of restenosis after percutaneous coronary intervention (PCI) [4]. As a well-characterized endogenous NO synthase inhibitor that can

☆ This study was supported by grants from the National Science Council, Taiwan, R.O.C. (NSC96-2314-B-075-071-MY3; MOST103-2314-B-075-046) and Taipei Veterans General Hospital, Taiwan, R.O.C. (V105C-098, V106C-184).

* Corresponding author at: Division of Cardiology, Department of Medicine, Taipei Veterans General Hospital, Taipei, Taiwan, ROC.
E-mail address: tmlu@vghtpe.gov.tw (T.-M. Lu).

https://doi.org/10.1016/j.ijcard.2019.05.003
0167-5273/

impair NO bioavailability and increase oxidative stress, asymmetric dimethylarginine (ADMA) has been suggested to be involved in the pathogenesis of atherosclerosis and endothelial dysfunction [5,6]. Indeed, previous studies have suggested that ADMA might independently predict the risk of subsequent ISR and major adverse cardiovascular events after PCI [7–9], suggested that ADMA might be involved in the pathogenesis of ISR.

Currently optical coherence tomography (OCT) with high resolution (10–20 μm) has been suggested to be a preferred imaging modality for the detailed in vivo assessment of ISR tissue characteristics, and may provide information helpful in elucidating the mechanisms of stent restenosis [10,11]. In this study, we aimed to evaluate the relation between the ISR lesions tissue morphologic and compositional characteristics evaluated by OCT and the plasma ADMA levels in patients developing ISR after coronary stenting.

2. Methods

2.1. Study design and objectives

We prospectively enrolled 45 consecutive patients with symptomatic angiographically documented ISR lesions (defined as diameter stenosis ≥50% by visual estimation in the vessel segment within the stent). Clinical exclusion criteria were acute decompensated congestive heart failure, acute and chronic infections, autoimmune diseases, malignancy with expected life span <1 year, and unstable hemodynamic status. Moreover, patients with left main ISR disease and in-stent total occlusion were also excluded. Our population included patients with stable angina ($n = 36$), unstable angina ($n = 5$) and non-ST segment elevation myocardial infarction ($n = 4$). All patients were screened for the protocol inclusion and exclusion criteria before enrolment. Thorough medical histories of all patients were recorded. All medications, cigarette smoking and beverages containing alcohol or caffeine were withdrawn for at least 12 h before blood sampling. Blood samples were collected before diagnostic coronary angiography, which was then performed by standard procedure. The study protocol was approved by the Institutional Review Board at Taipei-Veterans General Hospital, and all participants provided written informed consent.

2.2. Angiographic analysis

Coronary angiography was performed via the trans-radial or trans-femoral approach using 6 or 7 Fr. sheaths and catheter. The following angiographic parameters were obtained, including minimal lumen diameter (MLD, mm), reference vessel diameter (RVD, mm), and percentage diameter stenosis (%DS). We divided restenotic lesion type by angiography, using ISR classification by Mehran et al. [12], in "focal" and "diffuse".

2.3. Procedural details and OCT image acquisition and analysis

OCT pullback was performed using the ILUMIEN OPTIS™ system and Dragonfly™ (Abbott Vascular, Santa Clara, CA, USA) after an intracoronary injection of 400 μg of nitroglycerin. Automatic/manual pullbacks using contrast injection at a rate of 3 to 5 ml/s were performed with a motorized pullback speed of up to 36 mm/s, 180 frames per second, and a scan length of 54 mm. OCT images were analyzed by 2 independent investigators and OCT image analysis was performed offline using the ORW software (Abbott Vascular, Santa Clara, CA, USA) and OCT imaging was assessed at 1 mm intervals. We selected the frame with the most severe ISR, the following quantitative parameters were measured: MLD and minimal luminal area (MLA), stent area (mm^2), neo-intimal area ((stent area) – (MLA), mm^2) and stent length assessed by OCT imaging.

We measured the restenotic tissue in the region of MLA between the luminal contour and stent contour as intra-stent neointima. According to the OCT signal patterns, homogenous neointima was identified as signal-rich regions with low attenuation. Intra-stent calcified neointima was identified as a heterogeneous area with low signal attenuation and a sharply demarcated border. Intra-stent lipid neointima was defined as a homogeneous area with high signal attenuation and a diffuse border. As we found that there is nearly no ISR lesions without any minimal lipid or calcium in the whole stent, we defined neoatherosclerosis as ISR tissue with the presence of intra-stent lipid or calcified neointima with maximum lipid/calcium arc >90° [13]. Thin-cap fibroatheroma (TCFA) neointima was defined as lipid neointima with a fibrous cap thickness ≤65 μm at the thinnest part [14]. Quantitative analysis for the intra-stent calcium and lipid was performed using cross-sectional OCT images at 1-mm intervals, and calcium deposits were analyzed individually by measured calcium arc and length. We measured the intra-stent relative calcium index (RCI = (mean calcium arc × calcium length)/(360 × analyzed length)) and intra-stent relative lipid core index (RLCI = (mean lipid core arc × lipid core length)/(360 × analyzed length)) as the relative volumetric indices of in-stent calcium and lipid core content. A calcified nodule was defined as an accumulation of multiple small protruding nodular calcifications with superficial thrombus or fibrin [15,16]. Micro-vessel was defined as the well-delineated low backscattering structures <200 μm in diameter [10]. The Peri-strut Low Intensity Area (PLIA) was defined as a region around stent struts with homogeneous lower intensity than surrounding tissue, without signal attenuation [17]. Inter-observer and intra-observer variability were assessed by evaluating 20 randomly selected images for ISR angiographic classification (focal, diffuse). In-stent neointima characteristics (homogenous neointima, lipid neointima and calcified neointima), PLIA, RCI and RLCI by 2 independent expert readers (W—C H. and H—Y C.) and comparison by the same reader 2 weeks after the initial evaluation. Inter-observer and intra-observer reproducibility of image analyses were assessed by Kappa statistics for categorical variable or intraclass correlation coefficients (ICC) for continuous variable. There was good inter-observer and intra-observer agreement for the assessment of ISR angiographic classification (Kappa: 0.86, 0.91), in-stent neointima characteristics (Kappa: 0.81, 0.86), PLIA (Kappa: 0.86, 0.92), RCI (ICC: 0.91, 0.93) and RLCI (ICC: 0.89, 0.91).

2.4. Laboratory measurements

The blood samples were collected and were centrifuged at 3000 rpm for 10 min at 4 °C immediately. Plasma samples were kept frozen at −80 °C until analysis. Serum hypersensitivity-C-reactive protein (hs-CRP) was measured by an ultrasensitive nephelometric assay (DuoSet ELISA development kit; R&D Systems, Minneapolis, MN), with a lower detection limit of 0.2 mg/L. ADMA levels was measured by a competitive ELISA kits (DLD Diagnostika GmbH, Hamburg, Germany) with a standard range from 0.1 to 5.0 μmol/l. The detection limit is 0.05 μmol/l. Estimated glomerular filtration rate (eGFR) was calculated according to the MDRD formula [18]. Chronic kidney disease (CKD) was defined as eGFR ≤60 ml/min per 1.73 m^2.

2.5. Statistical analysis

All continuous data were presented as mean ± standard deviation or with 95% confidence interval (CI). The differences of continuous data between two groups were compared by two-sample *t*-test; the differences among three or more groups by analysis of variance (ANOVA). Post-Hoc comparisons were performed by Bonferroni test. Categorical data between two groups were compared by means of Chi-square test or Fisher's exact test. Pearson's correlation coefficients were calculated to examine possible correlations between continuous variables. Multivariate logistic/linear regression analyses were used to examine the association of plasma ADMA levels with ISR tissue characteristics assessed by OCT. A p value of <0.05 was considered to be statistically significant. All statistical analyses were performed using SPSS statistical software (IBM SPSS Statistics for Windows, Version 22.0. Armonk, NY: IBM Corp.).

3. Results

3.1. Baseline characteristics of the study population

Forty-five ISR lesions were evaluated by OCT in 45 patients, including 36 cases with stable angina, 5 with unstable angina, and 4 with non-ST elevation myocardial infarction. The mean age of was 69.5 ± 12.3 years, and most of the patients were male (38, 84.4%). ISR occurred in 17 BMSs, 12 1st-generation DESs (6 sirolimus-eluting cypher stent, 6 paclitaxel-eluting stent), and 16 2nd-generation DESs (limus-eluting stent). ISR occurred at a median period of 58.0 months after index stenting procedure (inter-quartile range: 14.5–97.0 months). The baseline clinical and angiographic characteristics are shown in Table 1.

The mean plasma ADMA level was 1.05 ± 0.22 μmol/l. Significant correlations were observed between plasma ADMA level and age ($r = 0.37$, $p = 0.012$), and eGFR ($r = -0.36$, $p = 0.015$), respectively. In addition, the plasma ADMA levels in patients with Mehran's classification diffuse type ISR ($n = 30$) were significantly higher than those of patients with focal type ISR ($n = 15$) (1.10 ± 0.22 μmol/l versus 0.95 ± 0.20 μmol/l, $p = 0.005$).

3.2. OCT features and plasma ADMA levels

The OCT data was summarized in Table 2. According to the findings of OCT, 12 (26.7%) and 33 (73.3%) ISR lesions were classified as with homogenous neointima and with neoatherosclerosis respectively. The patients with ISR lesions with neoatherosclerosis were older and had significantly worse renal function (Table 2). Notably, the patients with ISR neoatherosclerosis have significantly higher plasma ADMA levels compared to those of patients with homogenous neointima (1.12 ± 0.21 μmol/l versus 0.83 ± 0.08 μmol/l, $p < 0.001$, Fig. 1A). Moreover, patients with irregular ISR lumen shape had significantly higher plasma ADMA levels compared to patients with regular round ISR lumen (1.15 ± 0.24 μmol/l versus 0.98 ± 0.18 μmol/l, $p = 0.011$). PLIA was observed in 17 patients (37.8%), whose plasma ADMA levels

Table 1
Baseline characteristics.

Variables	Overall patients $N = 45$	Neoatherosclerosis (−) $N = 12$	Neoatherosclerosis (+) $N = 33$	p value	In-stent calcification (−) $N = 21$	In-stent calcification (+) $N = 24$	p value
Baseline characteristics							
Age, (year)	69.5 ± 12.3	61.5 ± 10.1	72.4 ± 11.9	0.007	63.7 ± 10.8	74.5 ± 11.4	0.002
Male	38 (84.4%)	11 (91.7%)	27 (81.8%)	0.420	19 (90.5%)	19 (57.6%)	0.296
Hypertension	39 (86.7%)	11 (91.7%)	28 (84.8%)	0.552	17 (81.0%)	22 (91.7%)	0.292
Diabetes	25 (55.6%)	7 (58.3%)	18 (54.5%)	0.821	13 (61.9%)	12 (50.0%)	0.423
Atrial fibrillation	6 (13.3%)	0 (0%)	6 (18.2%)	0.113	1 (4.8%)	5 (20.8%)	0.114
Hypercholesterolemia	26 (57.8%)	6 (50%)	20 (60.6%)	0.524	10 (47.6%)	16 (66.7%)	0.197
CKD	13 (28.9%)	0 (0%)	13 (39.4%)	0.010	3 (14.3%)	10 (41.7%)	0.043
Current smoker	3 (6.7%)	0 (0%)	3 (9.1%)	0.522	4 (19.0%)	5 (20.8%)	0.158
Ex-smoker	9 (20.0%)	3 (25.0%)	6 (18.2%)	0.688	3 (14.3%)	0 (0%)	0.112
History of old MI	8 (17.8%)	2 (16.7%)	6 (18.2%)	0.906	3 (14.3%)	5 (20.8%)	0.567
CHF	11 (24.4%)	4 (33.3%)	7 (21.1%)	0.403	6 (28.6%)	5 (20.8%)	0.547
Previous CABG	1 (2.2%)	0 (0%)	1 (3.1%)	0.542	0 (0%)	1(4.2%)	0.344
PAOD	4 (8.8%)	1(8.3%)	3 (9.1%)	0.937	2 (9.5%)	2 (8.4%)	0.889
Old stroke	1 (2.2%)	0 (0%)	1 (3.1%)	0.542	1 (4.8%)	0 (0%)	0.280
Clinical presentation				0.931			0.448
Stable angina	36 (80.0%)	10 (83.3%)	26 (78.8%)		18 (85.7%)	18 (75%)	
Unstable angina	5 (11.1%)	1 (8.3%)	4 (12.1%)		1 (4.8%)	4 (16.7%)	
NSTEMI	4 (8.9%)	1 (8.3%)	3 (9.1%)		2 (9.6%)	2 (8.3%)	
Medications, n (%)							
Aspirin	34 (75.6%)	10 (83.3%)	24 (72.7%)	0.464	17 (80.9%)	17 (70.8%)	0.431
Clopidogrel	14 (31.1%)	4 (33.3%)	12 (36.4%)	0.851	8 (38.1%)	8 (33.3%)	0.739
Beta-blocker	21 (46.7%)	7 (58.3%)	14 (42.4%)	0.388	8 (38.1%)	13 (54.2%)	0.323
ACEI/ARB	27 (60.0%)	7 (58.3%)	20 (60.6%)	0.372	12 (57.1%)	15 (62.5%)	0.546
Statins	20 (44.4%)	7 (58.3%)	13 (39.4%)	0.258	10 (47.6%)	10 (41.7%)	0.688
DAPT	10 (22.2%)	4 (33.3%)	6 (18.2%)	0.553	4 (19.1%)	5 (20.8%)	0.832
Laboratory measurements							
Total cholesterol (mg/dl)	156.6 ± 35.3	160.6 ± 40.2	155.2 ± 33.9	0.682	160.4 ± 38.2	153.2 ± 32.9	0.507
LDL-C (mg/dl)	89.5 ± 35.1	96.7 ± 37.1	87.2 ± 29.2	0.410	98.1 ± 33.1	83.5 ± 28.2	0.141
Creatinine (mg/dl)	2.04 ± 2.54	1.08 ± 0.20	2.39 ± 2.90	0.015	1.85 ± 2.31	2.19 ± 2.77	0.655
eGFR	61.4 ± 27.6	76.2 ± 15.4	56.1 ± 29.3	0.005	66.4 ± 25.4	57.1 ± 29.1	0.259
White blood cell (10^9/L)	6375 ± 1550	6708 ± 1875	6524 ± 1428	0.391	6566 ± 1704	6208 ± 1417	0.446
Left ventricular ejection fraction (%)	53.0 ± 11.1	56.3 ± 10.3	51.6 ± 11.3	0.946	52.7 ± 10.9	53.1 ± 11.4	0.908
Biomarkers							
ADMA (μmol/l)	1.05 ± 0.22	0.83 ± 0.08	1.12 ± 0.21	0.000	0.88 ± 0.11	1.19 ± 0.19	0.000
Hs-CRP (ng/mL)	3717 ± 8837	998.5 ± 1099	4700 ± 10,158	0.047	3155 ± 5880	4201 ± 10,899	0.697
Angiographic characteristics							
Stent type				0.086			0.203
BMS	17 (37.8%)	7 (58.3%)	10 (30.3%)		10 (47.6%)	7 (29.2%)	
DES	28 (62.2%)	5 (41.7%)	23 (69.7%)		11 (52.4%)	17 (70.8%)	
DES type				0.175			0.434
1ST-generation DES	12 (26.7%)	3 (25%)	9 (27.3%)		5 (23.8%)	7 (29.2%)	
2ND-generation DES	16 (35.6%)	2 (16.7%)	14 (42.4%)		6 (28.5%)	20 (83.3%)	
Duration of stent implantation (months)	58.0 (14.5–97.0)	63.5 ± 64	66 ± 52.8	0.894	64.0 ± 55.8	66.7 ± 56.0	0.872
Diseased vessel number				0.308			0.764
SVD	17 (37.8%)	5 (41.7%)	12 (36.4%)		9 (42.9%)	8 (33.3%)	
DVD	13 (28.9%)	5 (41.7%)	8 (24.2%)		6 (28.6%)	7 (29.2%)	
TVD	15 (33.3%)	2 (16.7%)	13 (39.4%)		6 (28.6%)	9 (37.5%)	
ISR angiographic classification				0.032			0.011
Focal	15 (33.3%)	7 (58.3%)	8 (24.2%)		11 (52.4%)	4 (16.7%)	
Diffuse	30 (66.7%)	5 (41.7%)	25 (75.8%)		10 (47.6%)	20(83.3%)	
QCA measurements							
MLD (mm)	1.41 ± 0.50	1.43 ± 0.36	1.39 ± 0.36	0.862	1.38 ± 0.22	1.44 ± 0.31	0.783
RVD (mm)	2.62 ± 0.51	2.58 ± 0.48	2.64 ± 0.31	0.831	2.60 ± 0.49	2.64 ± 0.56	0.854
DS (%)	78.6 ± 16.2	76.3 ± 17.1	82.1 ± 18.6	0.844	75.6 ± 18.6	81.3 ± 15.2	0.864

ADMA: asymmetric dimethylarginine; ACEI: angiotensin converting enzyme inhibitor; ARB: angiotensin-II receptor blocker; BMS: bare metal stents; CABG: coronary bypass grafting surgery; CHF: congestive heart failure; CKD: chronic kidney disease; DAPT: dual anti-platelet therapy; DES: drug-eluting stents; DS: diameter stenosis; DVD: double vessel disease; eGFR: estimated glomerular filtration rate; Hs-CRP: hypersensitivity C-reactive protein; ISR: in-stent restenosis; LDL-C: low density lipoprotein; MI: myocardial infarction; MLD: minimal lumen diameter; NSTEMI: non-ST segment elevation myocardial infarction; PAOD: peripheral artery occlusive disease; QCA: qualitative comparative analysis; RVD: reference vessel diameter; SVD: single vessel disease; TVD: triple vessel disease.

were significantly higher than those without (1.16 ± 0.25 μmol/l versus 0.98 ± 0.17 μmol/l, $p = 0.005$). Taken together, these evidences suggested that elevated ADMA levels might be involved in the development of neoatherosclerosis. In contrast, there was no significant association between plasma ADMA level and intra-stent neovascularization ($p = 0.302$).

In multivariate analysis adjusted for age, sex, diabetes, eGFR, plasma ADMA level remained the only significant predictor for the ISR lesions with neoatherosclerosis ($p = 0.008$, Table 3). Furthermore, the association of plasma ADMA level and ISR lesions with neoatherosclerosis remained significant after multi-variables adjustment either in BMS/DES group ($p = 0.041$, 0.052, respectively) or in

Table 2
Optical coherence tomography characteristics.

Variables	Overall patients N = 45	Neoatherosclerosis (−) N = 12	Neoatherosclerosis (−) N = 33	*p* value	In-stent Calcification (−) N = 21	In-stent Calcification (+) N = 24	*p* value
Quantitative parameters							
MLD (mm)	1.21 ± 0.37	1.19 ± 0.40	1.22 ± 0.36	0.851	1.19 ± 0.40	1.22 ± 0.33	0.755
MLA (mm^2)	2.47 ± 4.36	2.41 ± 4.22	2.62 ± 4.42	0.140	2.46 ± 4.22	2.51 ± 4.42	0.371
Neo-intimal area (mm^2)	3.69 ± 0.96	3.12 ± 0.64	3.90 ± 0.97	0.013	3.46 ± 0.86	3.89 ± 1.00	0.131
Mean calcium arc (degree)	115.4 ± 34.1	20.2 ± 2.25	121.4 ± 36.3	0.001	29.2 ± 28.5	145.5 ± 32.4	0.001
Mean calcium length (mm)	13.2 ± 4.12	7.81 ± 2.23	14.7 ± 3.42	0.000	7.92 ± 2.33	16.7 ± 3.12	0.000
Mean calcium thickness (mm)	0.46 ± 0.14	0.18 ± 0.04	0.58 ± 0.18	0.000	0.23 ± 0.11	0.69 ± 0.26	0.000
Mean lipid core arc (degree)	94.3 ± 54.9	29.6 ± 19.6	86.1 ± 38.1	0.000	76.6 ± 29.6	68.1 ± 18.1	0.452
RCI	0.14 ± 0.08.	0.07 ± 0.03	0.17 ± 0.07	0.000	0.09 ± 0.04	0.19 ± 0.07	0.000
RLCI	0.13 ± 0.08	0.05 ± 0.02	0.15 ± 0.08	0.000	0.13 ± 0.12	0.11 ± 0.02	0.407
Calcium nodule	9 (20.0%)	0 (0%)	9 (27.3%)	0.043	1 (4.8%)	8 (33.3%)	0.017
Lumen shape				0.215			0.038
Regular	27 (60.0%)	9 (75%)	18 (54.5%)		16 (76.2%)	11(45.8%)	
Irregular	18 (40.0%)	3 (25%)	15 (45.5%)		5 (23.8%)	13 (54.2%)	
Peri-strut low intensity area	17 (37.8%)	1 (8.3%)	16 (48.5%)	0.014	4 (19.0%)	11 (45.8%)	0.015
Total micro-vessels (Superficial, Deep)				0.667			0.889
Superficial	3 (6.7%)	1 (8.3%)	2 (6.1%)		1 (4.8%)	2 (9.6%)	
Deep	2 (4.4%)	1 (8.3%)	1 (3.1%)		1 (4.8%)	1 (4.8%)	

MLA: minimal lumen area; MLD: minimal lumen diameter; RCI: relative calcium index; RLCI: relative lipid core index.

lesions with ISR duration >36 months or ≤36 months, (n = 26/19, both $p < 0.01$, respectively).

3.3. ISR calcium/lipid and plasma ADMA levels

We also measured the intra-stent calcification parameters in OCT image. Extensive intra-stent calcification (calcium arc >90°) was presented in 24 lesions (53.3%, maximal calcium thickness: 0.71 ± 0.24 mm, mean calcium thickness: 0.46 ± 0.14 mm, mean calcium length: 13.2 ± 4.1 (mm), and mean calcification arc: 115.4 ± 34.1°), and patients with ISR lesions and calcified neointima were older and had worse renal function (Table 1). Calcium nodule was presented in 9 ISR lesions (20.0%). The presence of extensive intra-stent calcification was more common in patients with CKD ($p = 0.043$), but was not associated with ISR duration or stent type. In contrast, the plasma ADMA level of ISR lesions with extensive intra-stent calcification was significantly higher than those of ISR lesions without intra-stent calcification (1.19 ± 0.19 μmol/l versus 0.88 ± 0.11 μmol/l, $p < 0.001$, Fig. 1B). Likewise, the plasma ADMA level of ISR lesions with calcium nodule was also higher than those without (1.27 ± 0.17 μmol/l versus 0.99 ± 0.19 μmol/l, $p < 0.001$). In multivariate regression analysis, the plasma ADMA level significantly predicts the presence of intra-stent calcification as well as calcium nodule in ISR lesions ($p = 0.002$, $p = 0.019$, respectively). Furthermore, there was a highly significant association between plasma ADMA level and intra-stent RCI ($p < 0.001$, $r = 0.702$, Fig. 1C; multivariate-adjusted $p < 0.001$, Table 3). The association of plasma ADMA level and intra-stent RCI remained significant after multivariable adjustment either in BMS/DES group (both $p < 0.001$, respectively) or in lesions with ISR duration >36 months or ≤36 months (n = 26/19, both $p < 0.001$, respectively).

The plasma ADMA level was not correlated with RLCI in the whole population (correlation $p = 0.519$, $r = 0.10$). However, there was a highly significant association between plasma ADMA level and intra-stent RLCI in subgroup of patients without intra-stent calcification ($p = 0.004$, $r = 0.596$, multivariate adjusted $p = 0.022$, Fig. 1E). In contrast, there were no significant associations among plasma hs-CRP level/stent type/ISR duration and various ISR OCT parameters.

4. Discussion

4.1. Main findings

In this study, we find that the elevated plasma ADMA levels were associated with the presence of neoatherosclerosis in in-stent restenotic lesions. Moreover, plasma ADMA levels closely correlated with intra-stent calcification. Our findings provide the first evidence that ADMA might be involved in the development of ISR neoatherosclerosis and calcification.

4.2. ISR tissue pattern/composition characteristics and ADMA

Several studies have showed that ADMA might be associated with the risk of ISR after PCI [7–9], and the administration of L-arginine to antagonize the NO inhibitory effect by ADMA has been suggested to be beneficial in the prevention of ISR [19], though some studies showed negative results [20,21]. With high axial resolution (10–20 μm), OCT has been demonstrated to be able to detect different patterns of restenotic tissue after coronary stenting [10,22]. In-stent neoatherosclerosis is characterized by the lipid-laden neointima and/or calcification within the neointima by OCT imaging, and in this study we found that the plasma ADMA level was significant higher in ISR lesions with in-stent neoatherosclerosis compared to those of ISR lesions without. Although several clinical features, including longer duration of stent implantation, usage of DES and chronic kidney disease have been shown to be associated with the OCT-detected neoatherosclerosis [23], our study for the first time showed the relation between plasma ADMA level and in-stent neoatherosclerosis detected by OCT, and our findings were in line with previous small studies that showed the increased plasma ADMA levels might predict the risk of restenosis and adverse cardiovascular events after PCI [7–9]. On the other hand, PLIA has been reported to be correlated with the presence of fibrinoid and proteoglycans, and associated with neointimal proliferation after stenting [24]. Moreover, the presence of PLIA on OCT image might be associated with ISR and revascularization after everolimus-eluting stent implantation [25]. Therefore, it is interesting to find that ISR lesions with PLIA were associated with significantly higher plasma ADMA levels in this study. Nevertheless, the relation between ADMA and ISR tissue structure characteristics need to be confirmed in larger cohorts.

4.3. ADMA and ISR neoatherosclerosis – possible pathophysiologic mechanisms

Stent implantation causes severe injury of vascular endothelium, which is intrinsically repaired within several weeks to months. However, the process of re-endothelialization is often incomplete or dysfunctional, especially in DES, with poorly formed cell junctions, reduced expression of antithrombotic molecules and decreased NO

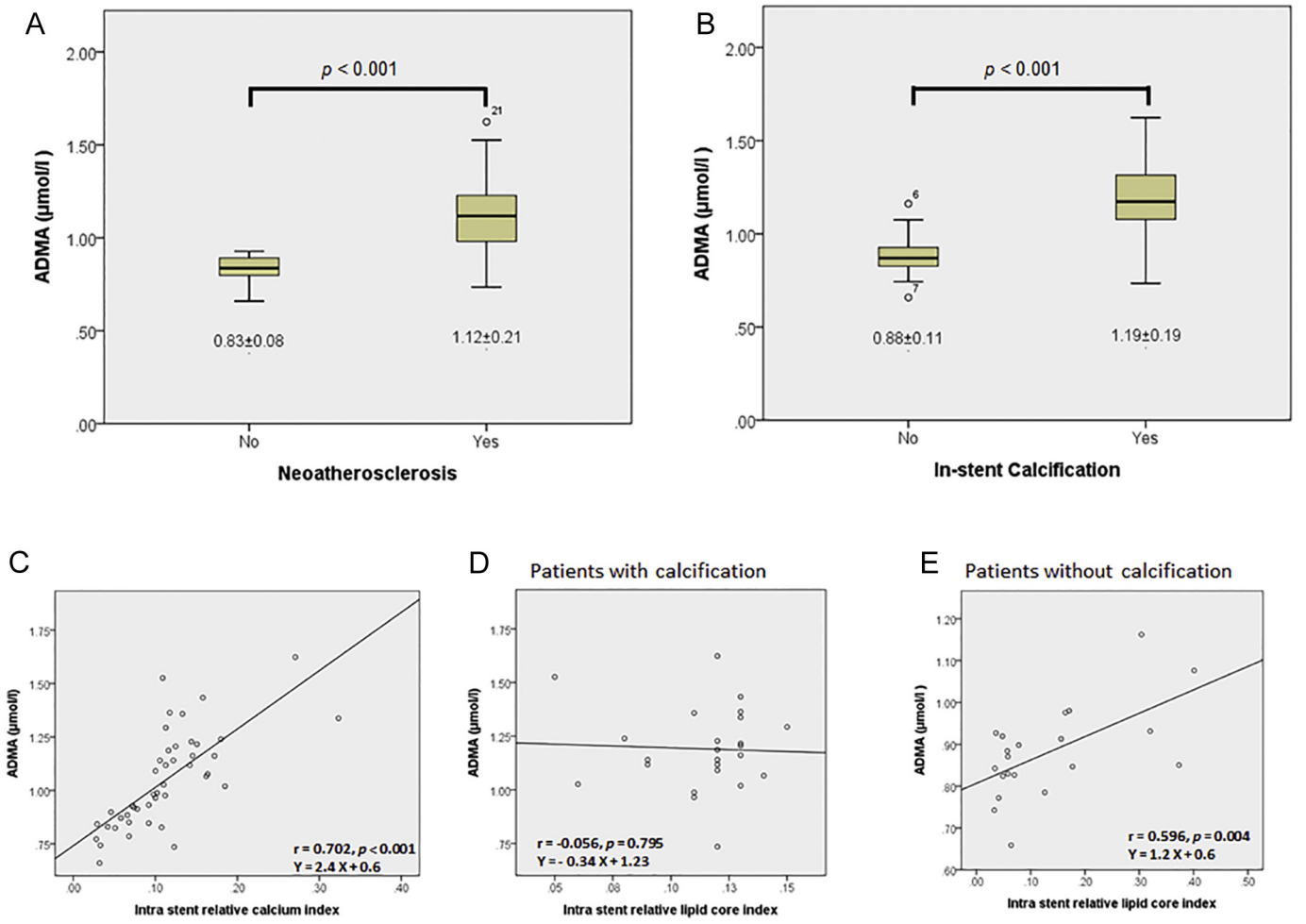

Fig. 1. A: Plasma ADMA levels according to the presence of neoatherosclerosis or not assessed by OCT. *p* values by Student's *t*-test are shown. B: Plasma ADMA levels according to the presence of intra-stent calcification or not assessed by OCT. *p* values by Student's t-test are shown. C–E: Correlations between plasma ADMA level and in-stent relative calcium index (RCI) in whole population (1C); and correlation between plasma ADMA level and in-stent relative lipid core index (RLCI) in patients with (1D) and without intra-stent calcification (1E). *p* values calculated by Pearson's correlation are shown.

production, and may lead to the development of very late in-stent thrombosis, neoatherosclerosis and restenosis [3]. Indeed, endothelial dysfunction, characterized by impaired NO bioavailability, is present in the initial stage of atherosclerosis and has been reported to predict the occurrence of ISR in patients undergoing PCI [26,27]. As an endogenous NO synthase inhibitor, ADMA was reported to be associated with endothelial dysfunction [5,6], probably via its effects on reducing NO bioavailability and/or increasing oxidative stress. Transgenic mice over-expressing dimethylarginine dimethylaminohydrolase 1 (DDAH1, the enzyme responsible for the degradation of ADMA in human) had lower plasma ADMA level, and was associated with accelerated endothelial regeneration and reduced neointimal hyperplasia after endothelial denudation and vascular injury [28]. ADMA was also independently associated with glycoprotein IIb/IIIa activation after stenting [29]. These evidences altogether suggested that ADMA might increase vascular superoxide formation, might be an endogenous atherogenic molecule, and might be involved in platelet activation, impaired vascular repair, formation of neoatherosclerosis and restenosis after coronary artery stenting.

4.4. Intra-stent calcification and ADMA

Coronary artery calcification has been regarded as a surrogate for total atherosclerotic plaque burden and may predict future adverse cardiovascular events [30]. Atherosclerotic plaque evolution, inflammation, and apoptosis of inflammatory cells may contribute to the initiation

Table 3
Multi-variable regression analyses for ISR lesions with neoatherosclerosis and in-stent calcification.

Variables	Neoatherosclerosis		In-stent RCI	
	Odds ratio (95% CI)	*p* value	Odds ratio (95% CI)	*p* value
Age	1.098 (0.973–1.239)	0.128	0.001 (0.000–0.003)	0.148
Sex	0.787 (0.029–21.288)	0.887	0.014 (−0.036–0.064)	0.578
Diabetes	0.458 (0.044–4.790)	0.514	−0.031 (−0.069–0.007)	0.111
ADMA (1 SD increase of ADMA)	25.218 (2.344–271.346)	0.008	0.048 (0.028–0.068)	<0.001
eGFR (1 SD increase of eGFR)	0.424 (0.088–2.051)	0.286	−0.004 (−0.024–0.068)	0.660

eGFR: estimated glomerular infiltration rate; RCI: relative calcium index.

and progression of coronary artery calcification [31], and ADMA may be involved in these processes, as ADMA has been reported to accelerate foam cell formation [32], and might induce apoptosis of endothelial cell by increasing intracellular oxidant production [33]. In the CARDIAC study, an independent relationship was found between plasma ADMA levels and the degree of coronary calcification detected by computer tomography [34]. Krzanowski M et al. recently reported that increased ADMA concentrations were related to medial arterial calcification and bone turnover parameters in patients with chronic kidney disease, suggested that ADMA might be involved in the development of advanced atherosclerosis and calcific atherosclerotic plaque [35]. In contrast, the incidence, characteristics and clinical implication of intra-stent neointimal calcification after stent implantation has rarely been addressed. An IVUS study has found that the neointimal calcification was presented only in 9.4% ISR lesions and was associated with impaired renal function and longer duration after stenting [36]. Recently, a OCT study showed that calcified neoatherosclerosis was the predominant pattern of ISR in 16% of ISR lesions, and was associated with older age, longer stent implantation period, less use of statins and angiotensin-converting enzyme inhibitors/angiotensin receptor blockers [37]. In contrast, we detected more intra-stent calcification in our ISR lesions (53.3%), which was associated with older age and worse renal function, but not with stent implantation duration or medication. These different findings might be related to the longer stent implantation duration and different demographic characteristics in our patients. Intriguingly, we found that there was a significant association between plasma ADMA levels and intra-stent RCI, independent on renal function, type of stent and duration of stent implantation. So far, few studies address the relation between ADMA and ISR calcification, and again, our results need to be confirmed in larger studies.

4.5. Limitations

There were several limitations in our study. First, the sample size of this study is relatively small, and including patients with stable angina and acute coronary syndrome, as well as patients undergoing PCI with implantation of BMS, 1st DES and 2nd DES. Moreover, there were large variations in the duration of ISR after index stenting procedure (median period of 58.0 months, inter-quartile range: 14.5–97.0 months). All these heterogeneities may lead to potential bias to this study, and our results may not be generalizable to other population, such as patients with left main ISR lesions, total occluded and bioresorbable scaffold (BVS) ISR lesions. In addition, the incidence of in-stent neoatherosclerosis of our study appeared to be higher than human autopsy study (DES: 23/38, 82%/BMS: 7/17, 59% in our study versus Nakazawa et al. DES 31%/BMS 16%) [1]. Longer implantation duration in our study might be a possible explanation, as the in-stent neoatherosclerosis would be more common as the stent was implanted for a longer duration. However, due to limited histopathological correlation studies with some tissue composition of the ISR lesions assessed by OCT remaining speculative, potential over-diagnosis of neoatherosclerosis by OCT could not be ruled out completely, and the limitations of tissue characterization with this technology should always need to be taken into consideration [38]. Finally, Khalifa et al. reported that ADMA levels might increase up to 30% 4 months following coronary stenting [39], suggesting that the temporal change of plasma ADMA levels may also be informative, but we did not measure the initial baseline plasma ADMA levels at the index PCI as well as after follow-up angiography to assess its predictive power for the follow-up OCT ISR tissue characteristics and the variation of plasma ADMA levels.

5. Conclusions

Increased plasma ADMA levels were associated with the development of ISR neoatherosclerosis and calcification. The role of ADMA in the pathogenesis of ISR after coronary stenting may warrant further studies.

Conflict of interest statement

The authors have no conflicts of interest to declare.

References

[1] G. Nakazawa, F. Otsuka, M. Nakano, M. Vorpahl, S.K. Yazdani, E. Ladich, F.D. Kolodgie, A.V. Finn, R. Virmani, The pathology of neoatherosclerosis in human coronary implants bare-metal and drug-eluting stents, J. Am. Coll. Cardiol. 57 (2011) 1314–1322.
[2] F. Otsuka, M. Vorpahl, M. Nakano, J. Foerst, J.B. Newell, K. Sakakura, R. Kutys, E. Ladich, A.V. Finn, F.D. Kolodgie, R. Virmani, Pathology of second-generation everolimus-eluting stents versus first-generation sirolimus- and paclitaxel-eluting stents in humans, Circulation. 129 (2014) 211–223.
[3] F. Otsuka, A.V. Finn, S.K. Yazdani, M. Nakano, F.D. Kolodgie, R. Virmani, The importance of the endothelium in atherothrombosis and coronary stenting, Nat. Rev. Cardiol. 9 (2012) 439–453.
[4] D.R. Janero, J.F. Ewing, Nitric oxide and postangioplasty restenosis: pathological correlates and therapeutic potential, Free Radic. Biol. Med. 29 (2000) 1199–1221.
[5] P. Vallance, A. Leone, A. Calver, J. Collier, S. Moncada, Accumulation of an endogenous inhibitor of nitric oxide synthesis in chronic renal failure, Lancet 339 (1992) 572–575.
[6] M. Juonala, J.S. Viikari, G. Alfthan, J. Marniemi, M. Kahonen, L. Taittonen, T. Laitinen, O.T. Raitakari, Brachial artery flow-mediated dilation and asymmetrical dimethylarginine in the cardiovascular risk in young Finns study, Circulation. 116 (2007) 1367–1373.
[7] T.M. Lu, Y.A. Ding, S.J. Lin, W.S. Lee, H.C. Tai, Plasma levels of asymmetrical dimethylarginine and adverse cardiovascular events after percutaneous coronary intervention, Eur. Heart J. 24 (2003) 1912–1919.
[8] H. Ari, S. Ari, E. Erdogan, O. Tiryakioglu, Y. Ustundag, K. Huysal, V. Koca, T. Bozat, A novel predictor of restenosis and adverse cardiac events: asymmetric dimethylarginine, Heart Vessel. 25 (2010) 19–26.
[9] A. Derkacz, M. Protasiewicz, R. Poreba, A. Doroszko, M. Poreba, J. Antonowicz-Juchniewicz, R. Andrzejak, A. Szuba, Plasma asymmetric dimethylarginine predicts restenosis after coronary angioplasty, Arch. Med. Sci. 7 (2011) 444–448.
[10] N. Gonzalo, P.W. Serruys, T. Okamura, H.M. van Beusekom, H.M. Garcia-Garcia, G. van Soest, W. van der Giessen, E. Regar, Optical coherence tomography patterns of stent restenosis, Am. Heart J. 158 (2009) 284–293.
[11] G.J. Tearney, E. Regar, T. Akasaka, T. Adriaenssens, P. Barlis, H.G. Bezerra, B. Bouma, N. Bruining, J.M. Cho, S. Chowdhary, M.A. Costa, R. de Silva, J. Dijkstra, C. Di Mario, D. Dudek, E. Falk, M.D. Feldman, P. Fitzgerald, H.M. Garcia-Garcia, N. Gonzalo, J.F. Granada, G. Guagliumi, N.R. Holm, Y. Honda, F. Ikeno, M. Kawasaki, J. Kochman, L. Koltowski, T. Kubo, T. Kume, H. Kyono, C.C. Lam, G. Lamouche, D.P. Lee, M.B. Leon, A. Maehara, O. Manfrini, G.S. Mintz, K. Mizuno, M.A. Morel, S. Nadkarni, H. Okura, H. Otake, A. Pietrasik, F. Prati, L. Raber, M.D. Radu, J. Rieber, M. Riga, A. Rollins, M. Rosenberg, V. Sirbu, P.W. Serruys, K. Shimada, T. Shinke, J. Shite, E. Siegel, S. Sonoda, M. Suter, S. Takarada, A. Tanaka, M. Terashima, T. Thim, S. Uemura, G.J. Ughi, H.M. van Beusekom, A.F. van der Steen, G.A. van Es, G. van Soest, R. Virmani, S. Waxman, N.J. Weissman, G. Weisz, International Working Group for Intravascular Optical Coherence T, Consensus standards for acquisition, measurement, and reporting of intravascular optical coherence tomography studies: a report from the International Working Group for Intravascular Optical Coherence Tomography Standardization and Validation, J. Am. Coll. Cardiol. 59 (2012) 1058–1072.
[12] R. Mehran, G. Dangas, A.S. Abizaid, G.S. Mintz, A.J. Lansky, L.F. Satler, A.D. Pichard, K.M. Kent, G.W. Stone, M.B. Leon, Angiographic patterns of in-stent restenosis: classification and implications for long-term outcome, Circulation 100 (1999) 1872–1878.
[13] E. Usui, T. Yonetsu, Y. Kanaji, M. Hoshino, M. Yamaguchi, M. Hada, R. Hamaya, Y. Kanno, T. Murai, T. Lee, K. Hirao, T. Kakuta, Prevalence of neoatherosclerosis in sirolimus-eluting stents in a very late phase after implantation, EuroIntervention. 14 (2018) e1316–e1323.
[14] K. Nakatsuma, H. Shiomi, T. Morimoto, K. Ando, K. Kadota, H. Watanabe, T. Taniguchi, T. Yamamoto, Y. Furukawa, Y. Nakagawa, M. Horie, T. Kimura, investigators CR-KA, Intravascular ultrasound guidance vs. angiographic guidance in primary percutaneous coronary intervention for ST-segment elevation myocardial infarction - long-term clinical outcomes from the CREDO-Kyoto AMI Registry, Circ. J. 80 (2016) 477–484.
[15] C.Y. Chin, M. Matsumura, A. Maehara, W. Zhang, C.T. Lee, M.H. Yamamoto, L. Song, Y. Parviz, N.B. Jhalani, S. Mohan, L.E. Ratner, D.J. Cohen, O. Ben-Yehuda, G.W. Stone, R.A. Shlofmitz, T. Kakuta, G.S. Mintz, Z.A. Ali, Coronary plaque characteristics in hemodialysis-dependent patients as assessed by optical coherence tomography, Am. J. Cardiol. 119 (2017) 1313–1319.
[16] T. Lee, G.S. Mintz, M. Matsumura, W. Zhang, Y. Cao, E. Usui, Y. Kanaji, T. Murai, T. Yonetsu, T. Kakuta, A. Maehara, Prevalence, predictors, and clinical presentation of a calcified nodule as assessed by optical coherence tomography, JACC Cardiovasc. Imaging 10 (2017) 883–891.
[17] H. Otake, J. Shite, F. Ikeno, T. Shinke, T. Teramoto, N. Miyoshi, J. Ako, Y. Honda, P.J. Fitzgerald, K. Hirata, Evaluation of the peri-strut low intensity area following sirolimus- and paclitaxel-eluting stents implantation: insights from an optical coherence tomography study in humans, Int. J. Cardiol. 157 (2012) 38–42.
[18] National Kidney F, K/DOQI clinical practice guidelines for chronic kidney disease: evaluation, classification, and stratification, Am. J. Kidney Dis. 39 (2002) S1–266.

[19] H.L. Gornik, M.A. Creager, Arginine and endothelial and vascular health, J. Nutr. 134 (2004) 2880S–2887S (discussion 2895S).
[20] L. Pleva, P. Kusnierova, P. Plevova, J. Zapletalova, M. Karpisek, L. Faldynova, P. Kovarova, P. Kukla, Increased levels of MMP-3, MMP-9 and MPO represent predictors of in-stent restenosis, while increased levels of ADMA, LCAT, ApoE and ApoD predict bare metal stent patency, Biomed. Pap. Med. Fac. Univ. Palacky Olomouc Czech Repub. 159 (2015) 586–594.
[21] K. Mizia-Stec, Z. Gasior, M. Haberka, M. Mizia, A. Chmiel, J. Janowska, M. Holecki, M. Mielczarek, B. Zahorska-Markiewicz, In-stent coronary restenosis, but not the type of stent, is associated with impaired endothelial-dependent vasodilatation, Kardiol. Pol. 67 (2009) 9–17 (discussion 18).
[22] K. Goto, H. Takebayashi, Y. Kihara, A. Hagikura, Y. Fujiwara, Y. Kikuta, K. Sato, S. Kodama, M. Taniguchi, S. Hiramatsu, S. Haruta, Appearance of neointima according to stent type and restenotic phase: analysis by optical coherence tomography, EuroIntervention. 9 (2013) 601–607.
[23] T. Yonetsu, K. Kato, S.J. Kim, L. Xing, H. Jia, I. McNulty, H. Lee, S. Zhang, S. Uemura, Y. Jang, S.J. Kang, S.J. Park, S. Lee, B. Yu, T. Kakuta, I.K. Jang, Predictors for neoatherosclerosis: a retrospective observational study from the optical coherence tomography registry, Circ. Cardiovasc. Imaging 5 (2012) 660–666.
[24] T. Teramoto, F. Ikeno, H. Otake, J.K. Lyons, H.M. van Beusekom, W.F. Fearon, A.C. Yeung, Intriguing peri-strut low-intensity area detected by optical coherence tomography after coronary stent deployment, Circ. J. 74 (2010) 1257–1259.
[25] K. Kuroda, H. Otake, T. Shinke, T. Toba, M. Kuroda, H. Takahashi, D. Terashita, K. Uzu, D. Kashiwagi, Y. Nagasawa, Y. Nagano, K.I. Hirata, Peri-strut low-intensity area assessed by mid-term follow-up optical coherence tomography may predict target lesion revascularization after everolimus-eluting stent implantation, EuroIntervention 14 (17) (2019) 1751–1759.
[26] G. Patti, V. Pasceri, R. Melfi, C. Goffredo, M. Chello, A. D'Ambrosio, R. Montesanti, G. Di Sciascio, Impaired flow-mediated dilation and risk of restenosis in patients undergoing coronary stent implantation, Circulation 111 (2005) 70–75.
[27] Y. Kitta, T. Nakamura, Y. Kodama, H. Takano, K. Umetani, D. Fujioka, Y. Saito, K. Kawabata, J.E. Obata, Y. Ichigi, A. Mende, K. Kugiyama, Endothelial vasomotor dysfunction in the brachial artery is associated with late in-stent coronary restenosis, J. Am. Coll. Cardiol. 46 (2005) 648–655.
[28] H. Konishi, K. Sydow, J.P. Cooke, Dimethylarginine dimethylaminohydrolase promotes endothelial repair after vascular injury, J. Am. Coll. Cardiol. 49 (2007) 1099–1105.
[29] T. Gremmel, T. Perkmann, C.W. Kopp, D. Seidinger, B. Eichelberger, R. Koppensteiner, S. Steiner, S. Panzer, Interleukin-6 and asymmetric dimethylarginine are associated with platelet activation after percutaneous angioplasty with stent implantation, PLoS One 10 (2015), e0122586.
[30] R. Wayhs, A. Zelinger, P. Raggi, High coronary artery calcium scores pose an extremely elevated risk for hard events, J. Am. Coll. Cardiol. 39 (2002) 225–230.
[31] T. Nakahara, M.R. Dweck, N. Narula, D. Pisapia, J. Narula, H.W. Strauss, Coronary artery calcification: from mechanism to molecular imaging, JACC Cardiovasc. Imaging 10 (2017) 582–593.
[32] I.V. Smirnova, M. Kajstura, T. Sawamura, M.S. Goligorsky, Asymmetric dimethylarginine upregulates LOX-1 in activated macrophages: role in foam cell formation, Am. J. Physiol. Heart Circ. Physiol. 287 (2004) H782–H790.
[33] D.J. Jiang, S.J. Jia, Z. Dai, Y.J. Li, Asymmetric dimethylarginine induces apoptosis via p38 MAPK/caspase-3-dependent signaling pathway in endothelial cells, J. Mol. Cell. Cardiol. 40 (2006) 529–539.
[34] C. Iribarren, G. Husson, K. Sydow, B.Y. Wang, S. Sidney, J.P. Cooke, Asymmetric dimethyl-arginine and coronary artery calcification in young adults entering middle age: the CARDIA Study, Eur J Cardiovasc Prev Rehabil. 14 (2007) 222–229.
[35] M. Krzanowski, K. Krzanowska, M. Gajda, P. Dumnicka, G. Kopec, B. Guzik, K. Woziwodzka, A. Dziewierz, J.A. Litwin, W. Sulowicz, Asymmetric dimethylarginine as a useful risk marker of radial artery calcification in patients with advanced kidney disease, Pol Arch Intern Med. 128 (2018) 157–165.
[36] Y. Kawase, J. Honye, H. Ota, T. Miyake, S. Kamikawa, H. Kondo, M. Okubo, K. Tsuchiya, H. Matsuo, I.K. Jang, K. Ueno, Neointimal calcification after stenting and chronic kidney disease, Int. Heart J. 54 (2013) 341–347.
[37] M. Garcia-Guimaraes, P. Antuna, R. Maruri-Sanchez, A. Vera, J. Cuesta, T. Bastante, F. Rivero, F. Alfonso, Calcified neoatherosclerosis causing in-stent restenosis: prevalence, predictors, and implications, Coron. Artery Dis. 30 (2019) 1–8.
[38] F. Otsuka, R.A. Byrne, K. Yahagi, H. Mori, E. Ladich, D.R. Fowler, R. Kutys, E. Xhepa, A. Kastrati, R. Virmani, M. Joner, Neoatherosclerosis: overview of histopathologic findings and implications for intravascular imaging assessment, Eur. Heart J. 36 (2015) 2147–2159.
[39] N.M. Khalifa, M.Z. Gad, A.A. Hataba, L.G. Mahran, Changes in ADMA and TAFI levels after stenting in coronary artery disease patients, Mol. Med. Rep. 6 (2012) 855–859.